ELSEVIER

Neurobiology of Aging 28 (2007) 1556–1567

NEUROBIOLOGY OF AGING

www.elsevier.com/locate/neuaging

Frontal connections and cognitive changes in normal aging rhesus monkeys: A DTI study

Nikos Makris [a,b,*], George M. Papadimitriou [a], Andre van der Kouwe [c], David N. Kennedy [a], Steven M. Hodge [a], Anders M. Dale [f], Thomas Benner [c], Lawrence L. Wald [c], Ona Wu [c], David S. Tuch [c], Verne S. Caviness [a], Tara L. Moore [b,d], Ronald J. Killiany [b,d], Mark B. Moss [b,d,e], Douglas L. Rosene [b,e]

[a] *Harvard Medical School Departments of Neurology and Radiology Services, Center for Morphometric Analysis, HST A. Martinos Center, Massachusetts General Hospital, Boston, MA 02129, United States*
[b] *Boston University School of Medicine, Department of Anatomy and Neurobiology, Boston, MA 02118, United States*
[c] *Harvard Medical School Departments of Neurology and Radiology Services, HST A. Martinos Center, Massachusetts General Hospital, Boston, MA 02129, United States*
[d] *Boston University School of Medicine, Department of Neurology, Boston, MA 02118, United States*
[e] *Emory University, Yerkes National Primate Research Center, Atlanta, GA 30322, United States*
[f] *Departments of Neurosciences, Radiology and Cognitive Neuroscience, UCSD, La Jolla, CA 92093, United States*

Received 7 November 2005; received in revised form 23 June 2006; accepted 6 July 2006
Available online 7 September 2006

Abstract

Recent anatomical studies have found that cortical neurons are mainly preserved during the aging process while myelin damage and even axonal loss is prominent throughout the forebrain. We used diffusion tensor imaging (DT-MRI) to evaluate the hypothesis that during the process of normal aging, white matter changes preferentially affect the integrity of long corticocortical association fiber tracts, specifically the superior longitudinal fasciculus II and the cingulum bundle. This would disrupt communication between the frontal lobes and other forebrain regions leading to cognitive impairments. We analyzed DT-MRI datasets from seven young and seven elderly behaviorally characterized rhesus monkeys, creating fractional anisotropy (FA) maps of the brain. Significant age-related reductions in mean FA values were found for the superior longitudinal fasciculus II and the cingulum bundle, as well as the anterior corpus callosum. Comparison of these FA reductions with behavioral measures demonstrated a statistically significant linear relationship between regional FA and performance on a test of executive function. These findings support the hypothesis that alterations to the integrity of these long association pathways connecting the frontal lobe with other forebrain regions contribute to cognitive impairments in normal aging. To our knowledge this is the first investigation reporting such alterations in the aging monkey.

Keywords: DT-MRI; Aging; White matter; Rhesus monkey

1. Introduction

Studies using non-human primate models of normal aging have provided evidence of a pattern of age-related cognitive decline in memory and executive function similar to humans (e.g. Albert and Moss [2] and Herndon [33]). Examinations of the brains of these behaviorally characterized young and old monkeys has demonstrated that cortical neurons are largely preserved in the cerebral cortex, including primary motor cortex (area 4), primary visual cortex (area 17), and prefrontal association cortex (area 46) (see Peters et al. [60] and Peters and Rosene [61]), while a variety of degenerative changes are

* Corresponding author at: Massachusetts General Hospital, Center for Morphometric Analysis, Building 149, 13th Street, Charlestown, MA 02129, United States. Tel.: +1 617 726 5733; fax: +1 617 726 5677.
E-mail address: nikos@cma.mgh.harvard.edu (N. Makris).

0197-4580/$ – see front matter © 2006 Elsevier Inc. All rights reserved.
doi:10.1016/j.neurobiolaging.2006.07.005

observed in forebrain white matter including myelin breakdown, loss of myelin and even mild loss of axons (e.g. Peters et al. [62], Sandell and Peters [79], and Peters and Rosene [61]). Anatomical studies in humans also indicate that neuron numbers are preserved in the cerebral cortex [29,32,55], while white matter is lost [44]. While these types of histological examinations are critical for examining the microstructures of the brain, because they are so labor intensive, they can only sample limited brain regions. In this regard, magnetic resonance imaging (MRI) offers a number of modalities that can provide global in vivo assessments of the various components of the brain such as the integrity of the white matter. In humans, MRI has been used to show an overall volume reduction in white matter in subjects ranging in age from 18 to 88 years [31]. When the same segmentation techniques were applied to the monkey, an overall decline in white matter volume is also detected [61] and morphological studies in humans and monkeys have confirmed a loss of white matter and myelinated axons [44,79]. Whether these changes in white matter reflect a ubiquitous change or a topographically specific process is unknown. To address this question we have employed Diffusion Tensor MRI (DT-MRI), which enables us to assess the integrity of white matter fibers by measuring the three-dimensional self-diffusion of water along the axons.

DT-MRI yields data on scalar metrics of fractional anisotropy (FA) and lattice anisotropy (LA). FA is the most commonly used of the two metrics [73]. FA is a calculated measure that is dependent on the orientational coherence of the diffusion compartments within a voxel. FA is thought to provide an index of the restrictional microstructure in the white matter and is measured in terms of its index. FA has a value of 0 for isotropic diffusion (e.g. minimally organized restriction in a single orientation, as in regions with crossing fibers) and a value of 1 for maximally anisotropic diffusion (e.g. maximally organized restriction in a single orientation, as in the internal capsule). Group differences in FA values of similar anatomical regions would suggest a difference in the white matter microenvironment. For example, lower fiber density or decreased orientation specificity would result in less tightly packed fiber bundles, and thus, water diffusion would be less restricted and FA values would be lower.

FA has been used to examine changes in white matter in multiple sclerosis [17], schizophrenia [39], alcoholism [69,71,72], amyotrophic lateral sclerosis [23], and other degenerative conditions in humans. Recent studies have also documented significant declines in the orientational organization of the white matter in normal and pathological aging, suggesting that DT-MRI may be a useful tool for the study of brain aging in humans [18,50,53,54,71,72,77,86]. However, there are no reported studies implementing DT-MRI in aging monkeys where both behavioral assessment and subsequent histological studies can be conducted and the present is the first study investigating FA differences in the white matter of aging rhesus monkeys.

We hypothesized that in aged monkeys, structural changes of long corticocortical association fiber tracts, specifically the superior longitudinal fasciculus II (SLF II) and the cingulum bundle (CB), but not projectional fiber tracts such as the corticospinal tract (ICpl), will produce decreases in their anisotropy that can be measured using DT-MRI. Based on behavioral findings that have been reported with aging monkeys suggesting declines in prefrontal functions [1,4,8,25,30,49], we expected anisotropy values within the frontal lobe white matter to be more severely affected. To test this hypothesis we acquired DT-MRI scans on seven young and seven aged rhesus monkeys that were behaviorally tested on tasks assessing recognition memory and executive function.

2. Methods

2.1. Subjects

The animals used for this study were obtained from the Yerkes Regional Primate Research Center at Emory University in Atlanta. They were selected according to strict health criteria designed to exclude any diseases, clinical, or experimental manipulations that might confound investigations of normal aging by adversely affecting the brain or behavior. These include any direct manipulations of the brain, history of chronic disease, history of immune system dysfunction, chronic drug treatments, major surgery such as splenectomy or thyroidectomy, or any manipulations of the endocrine system. They ranged in age from 7 to 31 years of age and with seven males and seven females distributed relatively equally across the range. An analysis of the life span in Yerkes colony by Tigges et al. [87] indicates that by about 16 years of age, half of all monkeys have died, that only about 25% live to 25 years of age and that the maximal life span for the rhesus monkey is around 35 years of age in captivity. Since monkeys reach sexual maturity between 4 and 5 years of age this suggests that the ratio of monkey to human age is approximately 1–3 so that if the relation is assumed to be linear, a 5-year-old monkey would correspond to a 15-year-old human, a 20-year-old monkey would correspond to a 60-year-old human, and a monkey over 30 would correspond to a human over 90. All procedures conformed to the guidelines of the U.S. Public Health Service Policy on Humane Care and Use of Laboratory Animals and were approved by Institutional Animal Care and Use Committees at the Yerkes Center, at Boston University Medical Center and at Massachusetts General Hospital. All facilities are fully accredited by the Association for the Assessment and Accreditation of Laboratory Animal Care.

2.2. Behavioral testing

As part of our studies of normal aging, all of the monkeys in this study were tested for about 9 months with a battery of behavioral tests assessing learning, recognition memory, attention, and executive function. As shown in Table 1, six of the seven young and all seven of the aged monkeys com-

Table 1
Animal characteristics and behavioral testing information

Animal number	Age	Gender	DNMS			DRST		CSST			
			Acq	2-min	10-min	Spatial	Object	IL	S1	S2	S3
AM129	6.5	F	+	+	+	+	+	−	−	−	−
AM131	6.5	F	−	−	−	−	−	−	−	−	−
AM127	7.0	M	+	+	+	+	+	+	+	+	+
AM132	7.0	M	+	+	+	+	+	+	+	+	+
AM130	7.5	F	+	+	+	+	+	−	−	−	−
AM144	14.5	M	+	+	+	+	+	+	+	+	+
AM143	15.0	M	+	+	+	+	+	+	+	+	+
AM124	19.5	M	+	+	+	+	+	+	+	+	+
AM133	19.5	M	+	+	+	+	+	+	+	+	+
AM125	20.0	F	+	+	+	+	+	−	−	−	−
AM126	20.5	F	+	+	+	+	+	+	+	+	+
AM123	20.5	M	+	+	+	+	−	+	+	+	+
AM120	26.5	F	−	+	−	+	+	−	−	−	−
AM119	30.5	F	+	+	+	+	+	−	−	−	−

F: female, M: male; animal was tested (+) or was not tested (−); DNMS: delayed non-match to sample (Acq: number of errors to criterion; 2-min: percent correct after 2 min delay; 10-min: percent correct after 10 min delay); DRST: delayed recognition span task (spatial: number correct, object: number correct); CSST: cognitive set shifting task (IL: number of errors to reach criterion during initial learning phase; S1: shift one errors to criterion; S2: shift two errors to criterion; S3: shift 3 errors to criterion).

pleted part or all of the behavioral test battery. The specific tasks included acquisition of the delayed non-match to sample (DNMS-Acq), a test of abstraction and rule learning, as well as DNMS performance at 2-min delays (DNMS-2) and at 10-min delays (DNMS-10) to test recognition memory. This was followed by two modalities of the Delayed Recognition Span Task, spatial (DRST-spt) and object (DRST-obj), which assess short-term memory capacity. Finally most subjects were then tested on a test of attention, followed by a simple three-choice discrimination task and then the Conceptual Set Shifting Task (CSST), a monkey version of the human Wisconsin Card Sort Test that assesses executive function. A detailed description of the implementation and assessment of performance on these tasks in monkeys is given in Herndon et al. [33] and Moore et al. [49]. A composite score for learning and memory that designated the cognitive impairment index (CII) was derived based on the principal components analysis of Herndon et al. [33], which indicated that overall impairments on the memory tasks were best predicted by a weighted average of each subject's scores on the DNMS-acq, the DNMS-2 and DRST-spt. To simplify this, scores on each of the three tasks for each subject were converted to a z-score relative to the mean performance of a baseline reference group of 40 young adults (5–10 years of age). The CII was then computed as a simple average of the three standardized scores with positive numbers indicating increasing impairments in z-units from the mean of the baseline reference group.

2.3. MRI scanning procedures

2.3.1. Animal preparation

At the conclusion of behavioral testing, monkeys underwent magnetic resonance imaging while tranquilized with ketamine and anesthetized with xylazine. For scanning the head was fixed in an MR compatible stereotactic frame [80], the ear bars aligned with the landmark and the monkey moved into the scanner where scans were acquired with the head fixed in the coronal stereotactic plane. No scans lasted longer than 15 min, allowing the monkey's anesthetic level to be assessed and adjusted at 15 min intervals without removing the monkey from the scanner and losing alignment. The anesthesia regimen provided stable anesthesia for 40–60 min, completely avoiding all movement artifacts.

2.3.2. Imaging

All monkeys received 3D T1-weighted anatomical (MP-RAGE) and diffusion-weighted (DT-MRI) imaging on a 1.5 T scanner (Siemens Sonata). The MP-RAGE scans were acquired with the following parameters: TR = 2730 ms, TE = 3.52 ms, TI = 1000 ms, flip angle = 7°, slice thickness = 1 mm, in-plane resolution = 0.78125 mm × 0.78125 mm, acquisition matrix = 256 × 256 (FOV = 200 mm × 200 mm), 4 repetitions of 128 contiguous sagittal slices, and pixel bandwidth = 190 Hz/pixel. The DT-MRI data was constructed by obtaining a seven-shot acquisition (T2 echo-planar or *lowb* with $b = 0$ s/mm^2, and six diffusion spatial encoding directions) with: TR = 130 ms, TE = 80 ms, TI = 80 ms, flip angle = 90°, NEX = 24, 40 coronal slices to cover the entire brain, slice thickness = 2 mm, skip = 1 mm, in-plane resolution = 1.328125 mm × 1.328125 mm, data matrix = 128 × 64 (FOV = 170 mm × 170 mm), bandwidth = 1220 Hz/pixel, diffusion sensitivity b = 600 s/mm^2, SNR approximately 60, and an imaging time of approximately 17 min.

2.4. DT-MRI analysis

This is an overview of our DT-MRI processing stream: (1) motion and eddy current distortion correction; (2) cor-

rected volume was used to generate fractional anisotropy (FA [73]) and apparent diffusion coefficient (ADC [74]) maps; (3) spatial transformation of each monkey's *lowb* to an average template created by co-registering (to a single subject) and averaging all *lowb* volumes; (4) FA and ADC maps were resampled using the transformation created by step (3); (5) spatial smoothing was applied to compensate for linear transformation limitations; (6) voxel-wise group statistics were generated based on the common-space smoothed FA and ADC data; (7) assessment of significant group differences in *a priori* defined anatomic regions, guided by statistical thresholding; (8) FA and ADC were calculated on the spatially normalized data of each monkey for the regions of significant difference, identified in the above step (7). Each of these steps is described in detail below.

2.4.1. Diffusion tensor calculations

For the DT-MRI data processing, we used a combination of the following processing streams: (a) Martinos Center FreeDiffusion Tools [77,78,88]; (b) FreeSurfer (http://surfer.nmr.mgh.harvard.edu/) [24]; (c) FSL (http://www.fmrib.ox.ac.uk/fsl) [36,37,83,84]; (d) MINC toolset from the Montreal Neurological Institute [19,20,47,91] (http://www.bic.mni.mcgill.ca/software/distribution).

The DT-MRI data were acquired as a seven-shot acquisition, that consisted of six directional volumes and a *lowb* structural with no diffusion weighting. All of the above was collected within the same sequence, and with identical parameters. A 12-degree affine mutual information cost function transformation (procedure available with FLIRT, FMRIB's Linear Image Registration Tool) was applied to all these volumes to help reduce eddy current distortions and motion along different repetitions (i.e., all 24 averages were aligned with the first *lowb* volume). Then, the diffusion tensor was calculated for each voxel in the volume, using a least-squares fit to the diffusion signal [9]. The fractional anisotropy was calculated from the diffusion tensor as in [73]. The resulting FA and ADC maps were resampled to an isotropic 1 mm^3 resolution using trilinear interpolation [77,78,88].

2.4.2. Spatial normalization

A *lowb* template was created by first registering each monkey to a randomly selected subject, and second averaging the normalized volumes. The FSL Brain Extraction Tool (BET) was previously used to skull-strip the input *lowb* volumes [83] to facilitate more uniform and precise registrations. These registrations were performed using the MINC toolset from the Montreal Neurological Institute; specifically a seven-parameter (three translations, three rotations, and a global scale) transformation was applied to each data set [19,20,47,91]. Each subject's *lowb* was subsequently registered to the average template using MINC as above. The FA and ADC maps were then spatially normalized to the common-space by using the transformations identified for their respective *lowb* volume. The transformed FA data were combined to create an overall average FA map (see Fig. 1).

2.4.3. Group maps

The spatially normalized FA and ADC maps were smoothed using a 3D spatial smoothing filter with a full width half maximum of 1.5 mm to compensate for possible imperfections in the co-registrations. Group analyses were performed to examine the regional distribution of diagnostic-group related changes in FA and ADC, by performing a voxel-based two-tailed *t*-test between the two diagnostic groups. The resultant statistical maps were thresholded at $p < 0.05$.

2.4.4. Anatomic regions of interest—FA values for individual subjects

Using the group average FA map we selected the following anatomical regions of interest (ROIs) to test our *a priori* hypothesis: (a) the superior longitudinal fasciculus II (SLF II), (b) the cingulum bundle (CB) and (c) the corticospinal tract at the posterior limb of the internal capsule (ICpl). The ICpl was selected as a control region where we did not expect any significantly different voxels to be encountered. In addition, for exploration we calculated the average FA value of the whole brain (including gray matter, white matter and CSF)

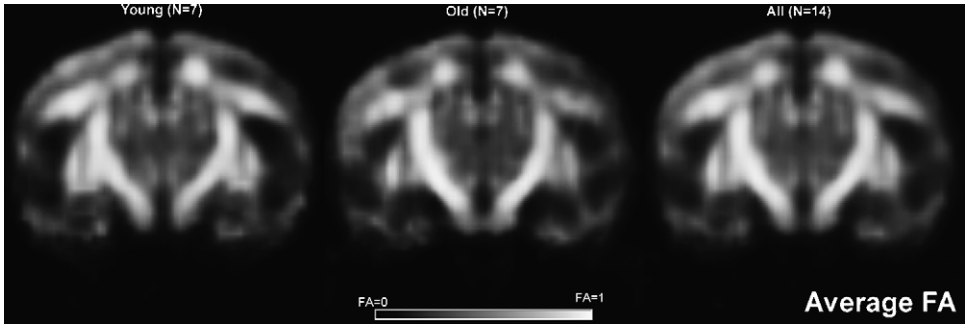

Fig. 1. Average fractional anisotropy (FA) maps of the young ($n = 7$) and old ($n = 7$) monkeys, as well as the combination (all 14 monkeys). FA provides an index of the restrictive microenvironment for water molecules in the white matter. It ranges from 0 to 1 and is lower in regions with minimally organized restriction in a single orientation (as in regions with crossing fibers) and higher in regions with maximally organized restriction in a single orientation (as in the internal capsule). Group differences in FA values of similar anatomical regions would suggest a difference in the white matter microenvironment.

and the anterior part of the corpus callosum (aCC), including the rostrum, genu and anterior third of the body. The locations of the anatomical ROIs were established based upon *a priori* knowledge of topographic anatomy from the experimental rhesus monkey literature. Because of the voxel size used in this DT-MRI study we were limited to investigating fiber bundles such as the SLF II, the CB, the ICpl and the aCC, which are sizeable enough to be detected. We limited our analysis to the portions of the fiber tracts where the axons course in compact bundles from origin to termination. These compact portions are called stems [40,42,43] and contain principally axons of a specific fiber tract as opposed to the corona radiata where such different types of axonal fibers as corticocortical, commissural and projectional coexist in variable but balanced proportions. Specifically, progressing through all the peri-callosal coronal sections, the voxels pertaining to the stem portions of the SLF II, CB, ICpl and aCC were determined by their location relative to other cerebral structures. This was done by one rater (NM) based on the mapping of these fiber pathways from known literature [52,56,64,65,82]. The regions were evaluated as follows (see Fig. 2). For SLF II, voxels in the region above the insula, the extreme capsule, the claustrum, the external capsule, the lenticular nucleus and the internal capsule were selected [64,65]. For the CB, voxels contained within the cingulate gyrus above the corpus callosum were selected [52]. For the ICpl, voxels within the internal capsule in the region between the lenticular nucleus laterally and the body of the caudate nucleus and thalamus medially were selected. For the aCC, voxels in the anterior third of the body as well as the genu and rostrum of the corpus callosum were selected. The ROIs were examined in each of the individuals to verify and guarantee the consistency and accuracy of their placement. This procedure generated average FA values for ROIs in both the right and left hemispheres in each subject, which then were summed across hemispheres to produce a bilateral mean FA value.

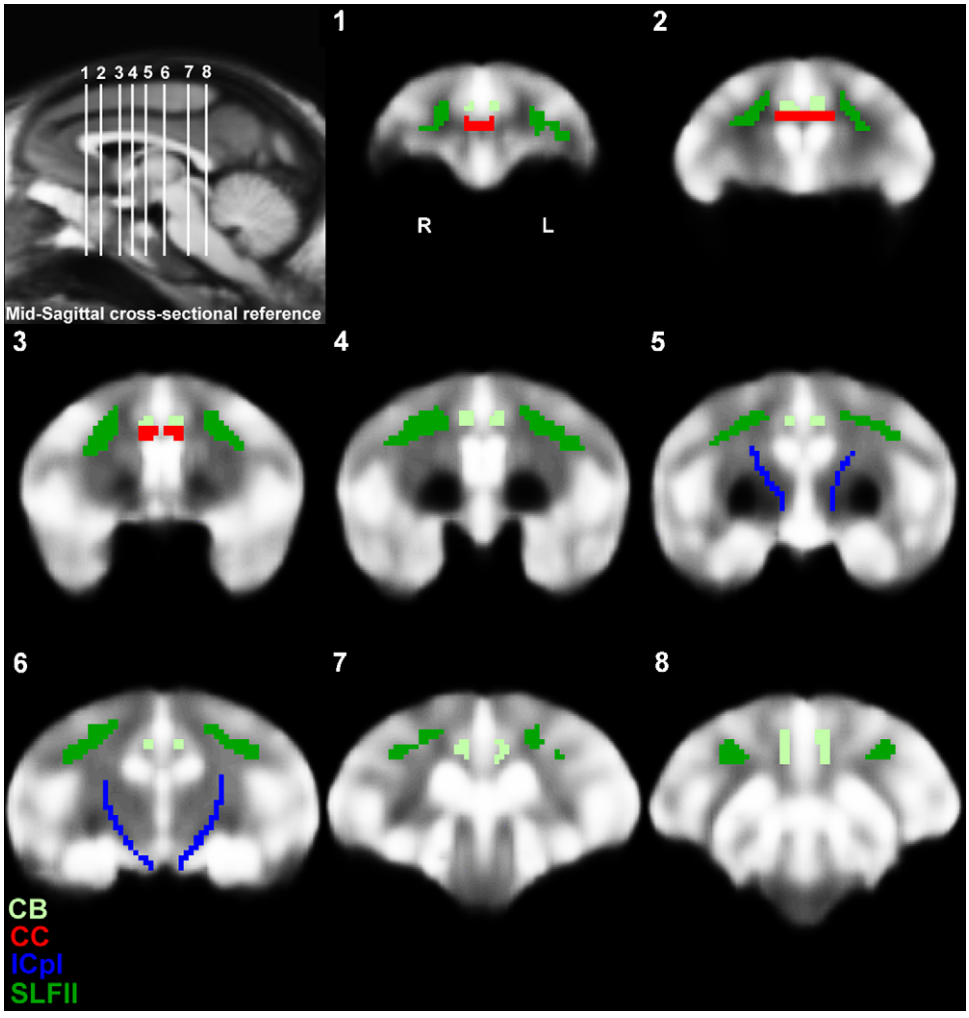

Fig. 2. Anatomical regions of interest (ROIs) in the monkey cerebrum for the superior longitudinal fascicle II (SLF II), the cingulum bundle (CB), the anterior part of the corpus callosum (aCC) and the posterior limb of the internal capsule (ICpl) in eight (1–8) representative coronal T2-EPI sections of the averaged monkey brain created from the individual T2-EPI datasets of all subjects ($n = 14$) that participated in the study displayed in the rostrocaudal dimension. The T1-weighted mid-sagittal section in the left upper corner indicates the levels of the coronal slices. The ROIs are color-coded. Abbreviations: aCC, anterior part of corpus callosum; CB, cingulum bundle; SLF II, superior longitudinal fasciculus II; L, left; R, right.

2.5. Brain tissue preservation

At the conclusion of behavioral testing and MRI scanning, monkeys were anesthetized and euthanized by exsanguination during perfusion of the brain to facilitate optimal preservation of brain tissue for future studies of MRI and anatomic relationships.

2.6. Statistical analyses

Analyses of FA data and behavioral data were done with monkeys stratified according to age so that monkeys ≤15 years of age were classified as young and those >15 were classified as old. FA maps were analyzed at two levels. First, average group maps were compared on a voxel by voxel basis using a two-tailed *t*-test. Second, individual bilateral mean FA values in *a priori* ROIs (SLF II, CB, ICpl) were compared between groups using a repeated measures ANOVA, followed by univariate tests of each ROI. Control for multiple comparisons was done using the method of Benjamini and Hochberg [10]. The data analyses were performed using the JMP statistical software package, version 5.0.1.2 (SAS Institute Inc., Carey, NC). The significance level was 0.05.

Exploratory analyses: individual mean FA values in other ROIs (the whole brain and the aCC) were examined with two-group *t*-tests. Scatter plots and regression analyses (Pearson correlations and partial correlations) were used to examine the relationship between mean FA values of the ROIs and performance on behavioral measures. Regression analyses were also performed to investigate the relative contribution of the association fiber bundles (SLF II and CB) versus a projectional fiber tract (the control ROI, ICpl) to performance on behavioral measures of executive function and recognition memory.

3. Results

3.1. Fractional anisotropy

The mean age of the young monkey group was 9.1 years (standard deviation (S.D.) = 3.9) and the mean age of the old monkey group was 22.4 years (S.D. = 4.3) [$t(12) = 6.1$, $p < 0.0001$]. The result of the inter-group difference FA maps for the young group ($n = 7$) versus the old group ($n = 7$) is shown in Fig. 3 and Table 2. Regions of significant (young greater than old) differences in FA signal fell entirely within the anatomical ROIs for SLF II, CB and aCC. No significant differences were observed in the ICpl, which was used as a control ROI. A repeated measures ANOVA showed a significant group by ROI interaction ($F(2, 11) = 4.3$, $p = 0.041$). As shown in Table 2, mean FA values for the ROIs of the SLF II and the CB were significantly higher in the young than in the old monkey group, but were not significantly different in the ICpl. Furthermore, mean FA values for the aCC were sig-

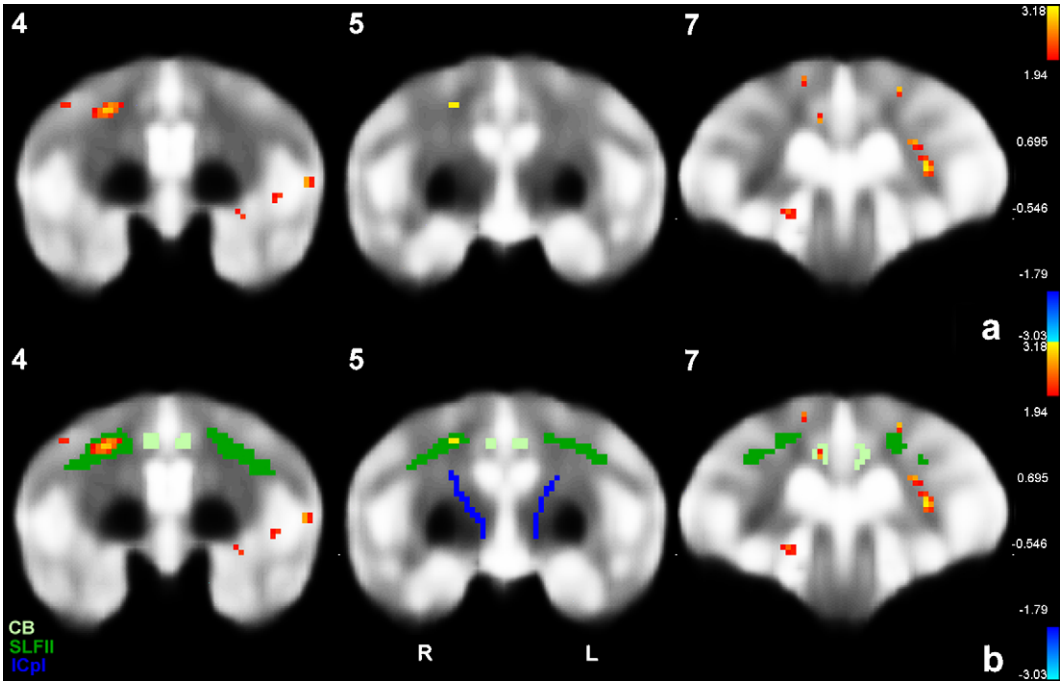

Fig. 3. (a) Inter-group difference FA maps in the monkey. Three representative coronal sections (4, 5 and 7 of Fig. 2) were used to overlay the fractional anisotropy (FA) group differences between young and old monkeys, which are shown in yellow and red. (b) Inter-group difference FA maps overlaid on the anatomical ROIs in three representative coronal sections (4, 5 and 7 of Fig. 2). The ROIs are color-coded. Abbreviations: aCC, anterior part of corpus callosum; CB, cingulum bundle; SLF II, superior longitudinal fasciculus II; L, left; R, right.

Table 2
Bilateral FA mapping data for two groups of monkeys: young (≤15 years) or old at time of scanning

FA map region	Mean ± S.D.		*t*-Test (d.f. = 12)
	Young	Old	
SLF II	0.48 ± 0.06	0.38 ± 0.07	−2.79*
CB	0.39 ± 0.06	0.30 ± 0.06	−2.86*
ICpl	0.49 ± 0.10	0.52 ± 0.08	0.64
Whole brain	0.25 ± 0.03	0.22 ± 0.04	−1.63
aCC	0.48 ± 0.11	0.37 ± 0.05	−2.31*

*$p < 0.05$, corrected for the false discovery rate using the method of Benjamini and Hochberg [10]; actual p-values are SLF II: 0.016, CB: 0.014, ICpl: 0.532. Abbreviations: FA, functional anisotropy; S.D., standard deviation; SLF II, superior longitudinal fasciculus; CB, cingulum bundle; ICpl, posterior limb of the internal capsule; aCC, anterior corpus callosum (rostrum + genu + anterior 1/3 body).

nificantly higher in the young than in the old monkey group (Table 2). There was not a significant group difference in the mean FA value of the whole brain.

3.2. Apparent diffusion coefficient

In each of the pathways studied, we measured the apparent diffusion coefficient (ADC) values in the young and old monkey groups. FA values were significantly negatively correlated with ADC values in each of the ROIs (range of r: −0.58 to −0.85; all $p < 0.0001$) except in the control region (ICpl $r = -0.34$, $p = 0.2$). ADC values ranged from 5.6×10^{-4} to 11.5×10^{-4} and no significant difference by group was observed. However, ADC values were higher in the old monkeys than in the young monkeys in the SLF II (old: 7.4×10^{-4}, young: 6.7×10^{-4}, $t(12) = 1.7$, $p = 0.1$), CB (old: 8.2×10^{-4}, young: 7.6×10^{-4}, $t(12) = 1.3$, $p = 0.2$), aCC (old: 9.3×10^{-4}, young: 9.2×10^{-4}, $t(12) = 0.2$, $p = 0.9$), and the ICpl (old: 7.7×10^{-4}, young: 7.7×10^{-4}, $t(12) = 0.1$, $p = 0.9$).

3.3. Behavioral correlations with fractional anisotropy

As shown in Fig. 4, there were significant negative correlations between FA values in the ROIs where there were significant group differences (y-axis) and a test of executive function, the number of errors committed on the acquisition phase of the CSST (x-axis) (SLF II: $r = -0.79$, $p = 0.02$; CB: $r = -0.74$, $p = 0.04$; aCC: $r = -0.79$, $p = 0.02$). These relationships were maintained, though moderated, even when the effect of age was partialled out (the partial correlations ranged from −0.66 to −0.67, p-values 0.098–0.104). In addition, we constructed regression models, which predicted the executive functioning score based on FA values of both the SLF II and the ICpl. The results indicate a significant contribution by the SLF II ($t(5) = -2.8$, $p = 0.04$) but not by the ICpl ($t(5) = 0.1$, $p = 0.9$). This same trend is seen when the aCC or CB is substituted for the SLF II. We did not find any correlations between FA values in our *a priori* ROIs and

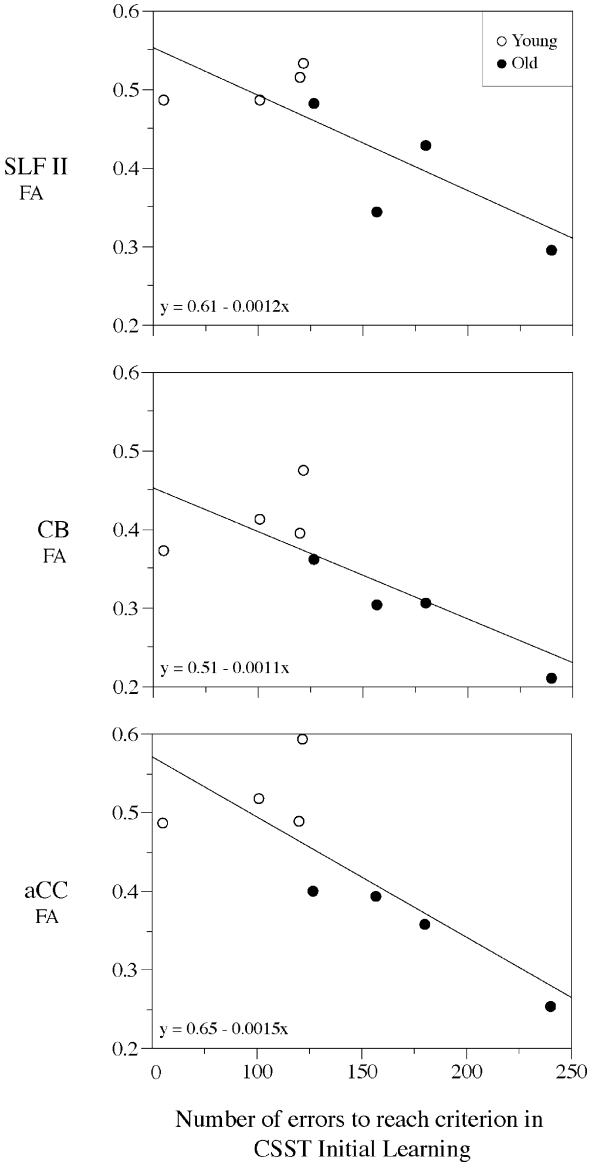

Fig. 4. Scatterplots showing the correlations between FA maps of bilateral regions of interest and the number of errors to reach criterion performance in the initial learning phase of the cognitive set shifting task (CSST). Linear regression lines are shown, as well as fitting equations. The plot symbols are distinct for the young and old monkey groups for display purposes only. These plots show a correlation of lower FA values in CB, SLF II and aCC associated with poorer performance. In addition, there is shown a separation between young and old monkeys indicating that this could be related to an age effect. Abbreviations: CB, cingulum bundle; SLF II, superior longitudinal fascicle II; aCC, anterior corpus callosum; CSST, cognitive set shifting task.

scores on the recognition memory tests. Furthermore, we did not find any group differences on these recognition memory tests. The plots in Fig. 4 show a correlation of lower FA values in SLF II, CB and aCC associated with poor performance in an executive function task. In addition, there is shown a differentiation between young and old monkeys. There were no significant correlations between FA values and scores on the recognition memory tasks.

4. Discussion

4.1. Summary

The process of normal aging in humans and monkeys is characterized by mild impairments in memory and executive function. Breakdown of the integrity of the myelin sheaths of axons has been observed in monkeys in frontal and temporal areas [60,62] and MRI studies have shown overall volume reduction in normal appearing white matter with segmentation procedures [61]. In this first study of FA differences in aging monkeys, we demonstrated that association cortico-cortical fiber pathways of the frontal lobe showed statistically significant reduced anisotropy in elderly rhesus monkeys. Specifically, the effect of aging has been observed in voxels placed over the regions representing the superior longitudinal fasciculus II (SLF II) and the cingulum bundle (CB). Moreover these changes in anisotropy correlated with performance on a test of executive function. These changes were not observed in such a control projection fiber bundle as the corticospinal tract (ICpl). In addition, exploratory analyses demonstrated significantly lower mean FA values for the anterior portion of the corpus callosum (aCC), which interconnects the right and left frontal lobes, and also lower mean FA values for the whole brain in the older group (but this was not statistically significant). Comparison of these FA reductions with behavioral measures demonstrated a statistically significant linear relationship between regional FA and performance on a test of executive function. No linear relationships were found with a test of recognition memory. Together these findings support the notion that during the process of normal aging white matter changes may affect corticocortical association pathways and the anterior part of the corpus callosum, thus disrupting the normal integration in the brain leading to impairments in cognitive function. Furthermore, it appears that alterations to the integrity of the long association cortico-cortical and callosal pathways of the frontal lobe contribute to impairments of executive function in normal aging.

4.2. Technical considerations

It is important to consider a number of technical limitations of this study. First, the subject pool, while stratified according to age, actually was quite heterogeneous and continuous and thus would work against finding group differences. Hence it would not be surprising to find significant changes in FA of other fiber pathways with a larger and/or more stratified population. Second, this study was done on a 1.5 T scanner, which limited the voxel size to 3.38 mm^3 (i.e., 1.3 mm × 1.3 mm × 2 mm), which is actually quite large relative to the monkey brain which has a total volume of around 100 cm^3 compared to human brain volumes in excess of 1200 cm^3. Hence, it is plausible that other smaller white matter bundles may show significant changes in FA when examined at 3.0 T where the sampling of smaller voxels is more feasible. Third, given the findings of white matter loss with age, voxels in the young and aged monkeys may contain differing amounts of the various pathways leading to different FA values. Fourth, there are statistical issues raised when performing voxel-based analyses across the entire brain volume. The issue of multiple comparisons is ameliorated in the selection of a limited number of anatomically circumscribed ROIs where data is pooled across the region. In this case, simple corrections for multiple comparisons are appropriate. In terms of the group maps of FA difference, the significance of regions showing statistically significant FA differences should be assessed in the context of the overall data smoothness (voxel to voxel spatial correlation) and the size of the spatially contiguous activation regions, such as used in Gaussian random field theory [38]. Fifth, the issue of multiple comparisons is also pertinent to the use of many behavioral tests for correlation with FA. We consider the bulk of behavioral correlation as *post hoc* comparisons, and accept some risk of elevated type I error, in that these behavioral correlations become *a priori* hypotheses for future studies. Finally, since individual subjects are averaged in a common space, the affine transformation that registers the individual to this space will not account for all individual anatomic variation. In this space, blurring on the order of 1 cm can be expected [20], requiring underlying significant regions to be large relative to this unaccounted for anatomic variance.

4.3. Functional role of frontal fiber tracts

DT-MRI provides the means to define the stems [42,43] of the different subcomponents of the superior longitudinal fasciculus [40], the cingulum bundle [41] and the corpus callosum [42], which are the major long associative fiber tracts connecting the frontal lobe to the rest of the cerebrum in the monkey and human cerebrum. Reviewing the functional role of these fiber systems will aid reasoning upon our observations on the FA changes of these fiber tracts in aging monkeys and their related impairment in executive function.

The SLF II, the main part of the SLF, is bidirectional connecting prefrontal regions implicated in working memory and executive functions [76] with the posterior parietal regions involved in visuospatial functions [3,13,14,28,35,46,51,75], as well as the superior temporal multimodal association regions. While the exact form of this interaction is unknown, possible functions may include focusing attention in different parts of space and/or to different aspects of incoming multimodal stimuli as part of working memory functions attributed to area 46 [15,76] and selecting between competing inputs on the basis of conditional rules established in the PFC, a function that is impaired in monkeys with lesions of area 8 [63,66].

The functional role of the cingulum bundle has been associated principally with the limbic system [58,92]. Fibers originating in the cingulate cortices project rostrally to the premotor and prefrontal cortices. Caudally they project to the posterior parietal cortices and project around the splenium of the corpus callosum to the parahippocampal gyrus. While the

exact function of the this complex bundle is unknown, the pattern of connections suggest a possible role of this fiber tract in the integration of visuospatial and motivational processes [57] as well as the memory functions of the limbic system including pain perception, motivation, emotion and visceral function [16,22,45].

The diverse functions of the corpus callosum have been derived from studies of humans with therapeutic callosal transections [11,21,26,27,85], clinical disturbances [59,81], and more recently by neuroimaging studies, which can detect and allow the study of individuals with traumatic damage to the callosum [90] as well as congenital agenesis of the callosum [59]. These studies demonstrate the importance of the callosum for interhemispheric integration of lateralized functions like language as well as for response inhibition (posterior corpus callosum [7]) and the control of spatial attention (anterior corpus callosum [90]). In this light, perhaps the FA changes in the aCC in our aging monkeys may contribute to age-related impairments in executive function [49].

4.4. Behavioral correlates

It is of interest that all three prefrontal lobe fiber bundles showed correlations with age-related impairments on a task of executive function. However, it is equally interesting that these FA changes were unrelated to impairments in recognition memory, suggesting that other factors might be critical, such as temporal lobe white matter, where changes may have been missed because of limitations of voxel size (i.e., the resolution of this study). Even more interesting is the fact that FA changes in these fiber tracts alone were not directly related to age-related impairments in rule learning (DNMS Acquisition), which may require both prefrontal and medial temporal lobe function but where such interaction may be subserved by the uncincate fasciculus rather than the arcuate fasciculus or the SLF II [82].

4.5. Further considerations

To our knowledge, other than the present study there is no other published DT-MRI study studying the process of white matter changes in normal, aging monkeys. On the other hand, there are several publications regarding white matter changes in the aging human brain in normality [12,50,54,77,78,86] and disease [5,17,23,34,39,48,67–72] as observed using the DT-MRI technique. The present results are generally agreeable with the observations in human aging populations. Specifically, studies conducted by different authors in aging humans [12,50,54,77,78,86] reported FA values for total brain white matter ranging from 0.24 to 0.45 for young and 0.22 to 0.39 in old, whereas our present results in monkeys were 0.25 in young versus 0.22 in old monkeys. Furthermore, these studies showed in young human populations FA values of 0.22–0.56 for white matter regions corresponding approximately to the SLF II and CB, 0.22–0.80 for the aCC and 0.22–0.66 for the ICpl. In old human populations, the same studies reported FA values of 0.22–0.55 for white matter regions corresponding approximately to the SLF II and CB, 0.20–0.71 for the aCC and 0.22–0.56 for the ICpl. Comparatively, our present results were 0.48 for SLF II, 0.39 for the CB, 0.48 for the aCC and 0.49 for the ICpl in young rhesus monkeys versus 0.38 for SLF II, 0.30 for the CB, 0.37 for the aCC and 0.52 for the ICpl in old rhesus monkeys. Moreover, in each of the pathways studied, we measured the apparent diffusion coefficient (ADC) values in the young and old monkey groups. While the ADC difference was not statistically significant between the two age groups, our ADC values in older animals were slightly larger than in young animals. Furthermore, ADC and FA were significantly negatively correlated in the all our regions of interest with the exception of the control region. The reason of our lack of significant differences in ADC between the two age groups may be due to the small sample size, to the regional specificity of our measurements, and the possibility that the aging effect in the monkey is smaller in magnitude than in humans [12,54].

The fiber pathways showing FA changes in our study shared a common quality, namely that they are long corticocortical association fiber tracts. Given that short association U-fibers are beyond the detectability of this method, we are unable to ascertain any changes in these fibers due to aging. This could be related to a common structural property of the long associative fiber systems that is different between the young and old monkey groups, and that reaches a magnitude sufficient for DT-MRI to detect. Thus besides being a systems aberration it could also be a pervasive abnormality reflecting something about the pathophysiology and molecular background in aging that causes this effect only where there is this special property of the associative fiber systems. Whereas in this study we tested hypotheses regarding a subset of relatively large (for our voxel size) association fiber pathways, which contribute heavily to the connectivity of the frontal lobe, future studies should investigate FA changes of all cerebral association fiber tracts. This will clarify further the notion whether FA alterations are situated within just the frontal lobe or more extensively, involving the associative systems of the entire cerebrum. Furthermore, we think that there should also be tested hypotheses related to alterations in the myelin content and myelin integrity of the association fiber systems. This seems plausible considering the fact that loss of myelin and structural alterations in myelin were observed in studies using light and electron microscopy (e.g. Peters et al. [62] and Sandell and Peters [79]). To this end, future studies should be conducted using other MRI modalities, such as magnetization transfer, which is more sensitive and more specific for detection of myelin changes [6,89].

5. Conclusions

Through their rich connections, the SLF II, the CB and the anterior callosal fiber systems constitute the major part of frontal lobe associational corticocortical ipsilateral and con-

tralateral (or commissural) connections. Alteration of these systems would affect the connectivity and functional integrity of the prefrontal cortex in the aging monkey. Behavioral correlations in our study support the idea that the cognitive functions of the prefrontal cortex in the old monkeys may be diminished as a consequence of changes in the integrity of the white matter as seen with DT-MRI.

Acknowledgements

This research was supported by the National Institute on Aging (1R03-AG20829-01), the National Center for Research Resources (P41-RR14075 and P51-RR00165), the National Association for Research in Schizophrenia and Depression (NARSAD), the Amyotrophic Lateral Sclerosis Association (ALSA), and the National Center for Complementary and Alternative Medicine (NCCAM) to Dr. Nikos Makris; the National Institute on Aging (P01-AG00001) to Dr. Douglas Rosene; BRP R01-EB00790-03 for Dr. Anders M. Dale; the Fairway Trust to Dr. David Kennedy; the Mental Illness and Neuroscience Discovery (MIND) Institute; the National Institute of Neurological Disorders and Stroke (NIH/NINDS 5R01NS38477) for Dr. One Wu; and the National Alliance for Medical Image Computing (National Institute for Biomedical Imaging and Bioengineering Grant U54 EB05149), which is funded through the National Institutes of Health Roadmap for Medical Research. The authors gratefully acknowledge Dr. Howard Cabral for his valuable assistance in the completion of this study and Dr. David Salat for useful discussions about the computation of Fractional Anisotropy maps.

References

[1] Albert M. Neuropsychological and neurophysiological changes in healthy adult humans across the age range. Neurobiol Aging 1993;14(6):623–5.
[2] Albert MS, Moss MB. Profiles of normal aging. In: Peters A, Morrison JH, editors. Neurodegenerative and age-related changes in the structure and function of cerebral cortex. Jones EG, Peters A, editors. Cerebral cortex, vol. 41. New York: Plenum Press; 1999.
[3] Andersen RA, Gnadt JW. Posterior parietal cortex. Rev Oculomot Res 1989;3:315–35.
[4] Arnsten AF, Contant TA. Alpha-2 adrenergic agonists decrease distractibility in aged monkeys performing the delayed response task. Psychopharmacology (Berl) 1992;108(1–2):159–69.
[5] Ashtari M, Kumra S, Bhaskar SL, Clarke T, Thaden E, Cervellione KL, et al. Attention-deficit/hyperactivity disorder: a preliminary diffusion tensor imaging study. Biol Psychiatry 2005;57(5):448–55.
[6] Balaban RS, Ceckler TL. Magnetization transfer contrast in magnetic resonance imaging. Magn Reson Q 1992;8(2):116–37.
[7] Barbeau E, Joubert S, Poncet M. A single case-study of diagonistic dyspraxia. Brain Cogn 2004;54(3):215–7.
[8] Bartus RT, Dean 3rd RL, Fleming DL. Aging in the rhesus monkey: effects on visual discrimination learning and reversal learning. J Gerontol 1979;34(2):209–19.
[9] Basser PJ, Mattiello J, LeBihan D. Estimation of the effective self-diffusion tensor from the NMR spin echo. J Magn Reson B 1994;103(3):247–54.
[10] Benjamini Y, Hochberg Y. Controlling the false discover rate: a practical and powerful approach to multiple testing. J R Statist Soc B 1995;57(1):289–300.
[11] Benowitz LI, Bear DM, Rosenthal R, Mesulam MM, Zaidel E, Sperry RW. Hemispheric specialization in nonverbal communication. Cortex 1983;19(1):5–11.
[12] Bhagat YA, Beaulieu C. Diffusion anisotropy in subcortical white matter and cortical gray matter: changes with aging and the role of CSF-suppression. J Magn Reson Imag 2004;20(2):216–27.
[13] Bisley JW, Goldberg ME. Neuronal activity in the lateral intraparietal area and spatial attention. Science 2003;299(5603):81–6.
[14] Bisley JW, Goldberg ME. The role of the parietal cortex in the neural processing of saccadic eye movements. Adv Neurol 2003;93:141–57.
[15] Brodmann K. Beitrage zur histologischen lokalisation der grosshirnrinde. III. Die rindenfelder der niederen affen. J Psychol Neurol 1905;4:177–226.
[16] Casey BJ, Trainor RJ, Orrendi JL, Schubert AB, Nystrom LE, Giedd JN, et al. A developmental functional MRI study of prefrontal activation during performance of a go-no-go task. J Cogn Neurosci 1997;9:835–47.
[17] Cercignani M, Iannucci G, Rocca MA, Comi G, Horsfield MA, Filippi M. Pathologic damage in MS assessed by diffusion-weighted and magnetization transfer MRI. Neurology 2000;54(5):1139–44.
[18] Charlton RA, Barrick TR, McIntyre DJ, Shen Y, O'Sullivan M, Howe FA, et al. White matter damage on diffusion tensor imaging correlates with age-related cognitive decline. Neurology 2006;66(2):217–22.
[19] Collignon A, Maes F, Delaere D, Vandermeulen D, Suetens P, Marchal G. Automated mulit-modality image registration based on information theory. Informat Process Med Imag 1995:263–74.
[20] Collins DL, Neelin P, Peters TM, Evans AC. Automatic 3D intersubject registration of MR volumetric data in standardized Talairach space. J Comput Assist Tomogr 1994;18(2):192–205.
[21] Devinsky O, Laff R. Callosal lesions and behavior: history and modern concepts. Epilepsy Behav 2003;4(6):607–17.
[22] Devinsky O, Morrell MJ, Vogt BA. Contributions of anterior cingulate cortex to behaviour. Brain 1995;118(Pt 1):279–306.
[23] Ellis CM, Simmons A, Jones DK, Bland J, Dawson JM, Horsfield MA, et al. Diffusion tensor MRI assesses corticospinal tract damage in ALS. Neurology 1999;53(5):1051–8.
[24] Fischl B, Salat DH, Busa E, Albert M, Dieterich M, Haselgrove C, et al. Whole brain segmentation: automated labeling of neuroanatomical structures in the human brain. Neuron 2002;33(3):341–55.
[25] Fristoe NM, Salthouse TA, Woodard JL. Examination of age-related deficits on the Wisconsin Card Sorting Test. Neuropsychology 1997;11(3):428–36.
[26] Gazzaniga MS. Cerebral specialization and interhemispheric communication: does the corpus callosum enable the human condition? Brain 2000;123(Pt 7):1293–326.
[27] Gazzaniga MS, Holtzman JD, Deck MD, Lee BC. MRI assessment of human callosal surgery with neuropsychological correlates. Neurology 1985;35(12):1763–6.
[28] Goldberg ME, Segraves MA. The visual and frontal cortices. Rev Oculomot Res 1989;3:283–313.
[29] Gomez-Isla T, Price JL, McKeel Jr DW, Morris JC, Growdon JH, Hyman BT. Profound loss of layer II entorhinal cortex neurons occurs in very mild Alzheimer's disease. J Neurosci 1996;16(14):4491–500.
[30] Gunning-Dixon FM, Raz N. The cognitive correlates of white matter abnormalities in normal aging: a quantitative review. Neuropsychology 2000;14(2):224–32.
[31] Guttmann CR, Jolesz FA, Kikinis R, Killiany RJ, Moss MB, Sandor T, et al. White matter changes with normal aging. Neurology 1998;50(4):972–8.
[32] Haug T. Are neurons of the human cerebral cortex really lost during aging? In: Traber J, Gispen WH, editors. Senile dementia of the Alzheimer's type. Berlin: Springer-Verlag; 1985. p. 150–63.
[33] Herndon JG, Moss MB, Rosene DL, Killiany RJ. Patterns of cognitive decline in aged rhesus monkeys. Behav Brain Res 1997;87(1):25–34.

[34] Hoptman MJ, Ardekani BA, Butler PD, Nierenberg J, Javitt DC, Lim KO. DTI and impulsivity in schizophrenia: a first voxelwise correlational analysis. Neuroreport 2004;15(16):2467–70.
[35] Hyvarinen J, Shelepin Y. Distribution of visual and somatic functions in the parietal associative area 7 of the monkey. Brain Res 1979;169(3):561–4.
[36] Jenkinson M, Bannister P, Brady M, Smith S. Improved optimization for the robust and accurate linear registration and motion correction of brain images. Neuroimage 2002;17(2):825–41.
[37] Jenkinson M, Smith S. A global optimisation method for robust affine registration of brain images. Med Image Anal 2001;5(2):143–56.
[38] Kiebel SJ, Poline JB, Friston KJ, Holmes AP, Worsley KJ. Robust smoothness estimation in statistical parametric maps using standardized residuals from the general linear model. Neuroimage 1999;10(6):756–66.
[39] Kubicki M, Westin CF, Maier SE, Mamata H, Frumin M, Ersner-Hershfield H, et al. Diffusion tensor imaging and its application to neuropsychiatric disorders. Harv Rev Psychiatry 2002;10(6): 324–36.
[40] Makris N, Kennedy DN, McInerney S, Sorensen AG, Wang R, Caviness Jr VS, et al. Segmentation of subcomponents within the superior longitudinal fascicle in humans: a quantitative, in vivo, DT-MRI study. Cereb Cortex 2005;15(6):854–69.
[41] Makris N, Pandya DN, Normandin JJ. Quantitative DT-MRI investigations of the human cingulum bundle. CNS Spectr 2002;7(7):522–8.
[42] Makris N, Papadimitriou GM, Worth AJ, Jenkins BG, Garrido L, Sorensen AG, et al. Diffusion Tensor Imaging. In: Davis KL, Charney D, Coyle J, Nemeroff C, editors. Neuropsychopharmacology: the fifth generation of progress. New York: Lippincott, Williams, and Wilkins; 2002. p. 357–71.
[43] Makris N, Worth AJ, Sorensen AG, Papadimitriou GM, Wu O, Reese TG, et al. Morphometry of in vivo human white matter association pathways with diffusion-weighted magnetic resonance imaging. Ann Neurol 1997;42(6):951–62.
[44] Marner L, Nyengaard JR, Tang Y, Pakkenberg B. Marked loss of myelinated nerve fibers in the human brain with age. J Comp Neurol 2003;462(2):144–52.
[45] Mesulam M-M. Behavioral neuroanatomy. large-scale networks, association cortex, frontal syndromes, the limbic system, and hemispheric specializations. In: Mesulam M-M, editor. Principles of behavioral and cognitive neurology. 2nd ed. Oxford: Oxford University Press; 2000. p. 1–120.
[46] Mesulam MM. A cortical network for directed attention and unilateral neglect. Ann Neurol 1981;10(4):309–25.
[47] Minoshima S, Berger KL, Lee KS, Mintun MA. An automated method for rotational correction and centering of three-dimensional functional brain images. J Nucl Med 1992;33(8):1579–85.
[48] Moeller FG, Hasan KM, Steinberg JL, Kramer LA, Dougherty DM, Santos RM, et al. Reduced anterior corpus callosum white matter integrity is related to increased impulsivity and reduced discriminability in cocaine-dependent subjects: diffusion tensor imaging. Neuropsychopharmacology 2005;30(3):610–7.
[49] Moore TL, Killiany RJ, Herndon JG, Rosene DL, Moss MB. Impairment in abstraction and set shifting in aged rhesus monkeys. Neurobiol Aging 2003;24(1):125–34.
[50] Moseley M. Diffusion tensor imaging and aging—a review. NMR Biomed 2002;15(7–8):553–60.
[51] Mountcastle VB, Lynch JC, Georgopoulos A, Sakata H, Acuna C. Posterior parietal association cortex of the monkey: command functions for operations within extrapersonal space. J Neurophysiol 1975;38(4):871–908.
[52] Mufson EJ, Pandya DN. Some observations on the course and composition of the cingulum bundle in the rhesus monkey. J Comp Neurol 1984;225(1):31–43.
[53] Nusbaum AO, Tang CY, Buchsbaum MS, Wei TC, Atlas SW. Regional and global changes in cerebral diffusion with normal aging. AJNR Am J Neuroradiol 2001;22(1):136–42.
[54] O'Sullivan M, Jones DK, Summers PE, Morris RG, Williams SC, Markus HS. Evidence for cortical "disconnection" as a mechanism of age-related cognitive decline. Neurology 2001;57(4):632–8.
[55] Pakkenberg B, Gundersen HJ. Neocortical neuron number in humans: effect of sex and age. J Comp Neurol 1997;384(2):312–20.
[56] Pandya DN, Rosene DL. Some observations on trajectories and topography of commissural fibers. In: Reeves AG, editor. Epilepsy and the corpus callosum. New York, NY: Plenum Publishing Corporation; 1985. p. 21–39.
[57] Pandya DN, Yeterian EH. Architecture and connections of cortical association areas. In: Peters A, Jones EG, editors. Association and auditory cortices. cerebral cortex, vol. 4. New York: Plenum Press; 1985. p. 3–61.
[58] Papez JW. A proposed mechanism of emotion. Arch Neurol Psychiatry 1937;38:725–43.
[59] Paul LK, Schieffer B, Brown WS. Social processing deficits in agenesis of the corpus callosum: narratives from the Thematic Appreciation Test. Arch Clin Neuropsychol 2004;19(2):215–25.
[60] Peters A, Morrison JH, Rosene DL, Hyman BT. Feature article: are neurons lost from the primate cerebral cortex during normal aging? Cereb Cortex 1998;8(4):295–300.
[61] Peters A, Rosene DL. In aging, is it gray or white? J Comp Neurol 2003;462(2):139–43.
[62] Peters A, Rosene DL, Moss MB, Kemper TL, Abraham CR, Tigges J, et al. Neurobiological bases of age-related cognitive decline in the rhesus monkey. J Neuropathol Exp Neurol 1996;55(8):861–74.
[63] Petrides M. The effect of periarcuate lesions in the monkey on the performance of symmetrically and asymmetrically reinforced visual and auditory go, no-go tasks. J Neurosci 1986;6(7):2054–63.
[64] Petrides M, Pandya DN. Projections to the frontal cortex from the posterior parietal region in the rhesus monkey. J Comp Neurol 1984;228(1):105–16.
[65] Petrides M, Pandya DN. Association fiber pathways to the frontal cortex from the superior temporal region in the rhesus monkey. J Comp Neurol 1988;273(1):52–66.
[66] Petrides M, Pandya DN. Comparative cytoarchitectonic analysis of the human and the macaque ventrolateral prefrontal cortex and corticocortical connection patterns in the monkey. Eur J Neurosci 2002;16(2):291–310.
[67] Pfefferbaum A, Adalsteinsson E, Sullivan EV. Frontal circuitry degradation marks healthy adult aging: evidence from diffusion tensor imaging. Neuroimage 2005;26(3):891–9.
[68] Pfefferbaum A, Adalsteinsson E, Sullivan EV. Supratentorial profile of white matter microstructural integrity in recovering alcoholic men and women. Biol Psychiatry 2006;59(4):364–72.
[69] Pfefferbaum A, Sullivan EV. Microstructural but not macrostructural disruption of white matter in women with chronic alcoholism. Neuroimage 2002;15(3):708–18.
[70] Pfefferbaum A, Sullivan EV. Disruption of brain white matter microstructure by excessive intracellular and extracellular fluid in alcoholism: evidence from diffusion tensor imaging. Neuropsychopharmacology 2005;30(2):423–32.
[71] Pfefferbaum A, Sullivan EV, Hedehus M, Adalsteinsson E, Lim KO, Moseley M. In vivo detection and functional correlates of white matter microstructural disruption in chronic alcoholism. Alcohol Clin Exp Res 2000;24(8):1214–21.
[72] Pfefferbaum A, Sullivan EV, Hedehus M, Lim KO, Adalsteinsson E, Moseley M. Age-related decline in brain white matter anisotropy measured with spatially corrected echo-planar diffusion tensor imaging. Magn Reson Med 2000;44(2):259–68.
[73] Pierpaoli C, Basser PJ. Toward a quantitative assessment of diffusion anisotropy. Magn Reson Med 1996;36(6):893–906 [published erratum appears in Magn Reson Med 1996;37(6):972].
[74] Pierpaoli C, Jezzard P, Basser PJ, Barnett A, Di Chiro G. Diffusion tensor MR imaging of the human brain. Radiology 1996;201(3):637–48.
[75] Posner MI, Walker JA, Friedrich FJ, Rafal RD. Effects of parietal injury on covert orienting of attention. J Neurosci 1984;4(7):1863–74.

[76] Preuss TM, Goldman-Rakic PS. Connections of the ventral granular frontal cortex of macaques with perisylvian premotor and somatosensory areas: anatomical evidence for somatic representation in primate frontal association cortex. J Comp Neurol 1989;282(2):293–316.
[77] Salat DH, Tuch DS, Greve DN, van der Kouwe AJ, Hevelone ND, Zaleta AK, et al. Age-related alterations in white matter microstructure measured by diffusion tensor imaging. Neurobiol Aging 2005;26(8):1215–27.
[78] Salat DH, Tuch DS, Hevelone ND, Fischl B, Corkin S, Rosas HD, et al. Age-related changes in prefrontal white matter measured by diffusion tensor imaging. Ann NY Acad Sci 2005;1064:37–49.
[79] Sandell JH, Peters A. Disrupted myelin and axon loss in the anterior commissure of the aged rhesus monkey. J Comp Neurol 2003;466(1):14–30.
[80] Saunders RC, Aigner TG, Frank JA. Magnetic resonance imaging of the rhesus monkey brain: use for stereotactic neurosurgery. Exp Brain Res 1990;81(2):443–6.
[81] Scepkowski LA, Cronin-Golomb A. The alien hand: cases, categorizations, and anatomical correlates. Behav Cogn Neurosci Rev 2003;2(4):261–77.
[82] Schmahmann JD, Pandya DN. Fiber pathways of the brain. New York: Oxford University Press; 2006.
[83] Smith SM. Fast robust automated brain extraction. Hum Brain Mapp 2002;17(3):143–55.
[84] Smith SM, De Stefano N, Jenkinson M, Matthews PM. Normalized accurate measurement of longitudinal brain change. J Comput Assist Tomogr 2001;25(3):466–75.
[85] Sperry R. Consciousness, personal identity and the divided brain. Neuropsychologia 1984;22(6):661–73.
[86] Sullivan EV, Adalsteinsson E, Hedehus M, Ju C, Moseley M, Lim KO, et al. Equivalent disruption of regional white matter microstructure in ageing healthy men and women. Neuroreport 2001;12(1):99–104.
[87] Tigges J, Gordon TP, McClure HM, Hall EC, Peters A. Survival rate and lifespan of rhesus monkeys at the Yerkes Regional Primate Research Center. Am J Primat 1988;15(3):263–73.
[88] Tuch DS, Salat DH, Wisco JJ, Zaleta AK, Hevelone ND, Rosas HD. Choice reaction time performance correlates with diffusion anisotropy in white matter pathways supporting visuospatial attention. Proc Natl Acad Sci USA 2005;102(34):12212–7.
[89] Wolff SD, Balaban RS. Magnetization transfer imaging: practical aspects and clinical applications. Radiology 1994;192(3):593–9.
[90] Wolk DA, Coslett HB. Hemispheric mediation of spatial attention: pseudoneglect after callosal stroke. Ann Neurol 2004;56(3):434–6.
[91] Woods RP, Mazziotta JC, Cherry SR. MRI-PET registration with automated algorithm. J Comput Assist Tomogr 1993;17(4):536–46.
[92] Yakovlev PI, Locke S. Limbic nuclei of thalamus and connections of limbic cortex. III. Corticocortical connections of the anterior cingulate gyrus, the cingulum, and the subcallosal bundle in monkey. Arch Neurol 1961;5:364–400.